RESEARCH ARTICLE

A Systematic Approach of Generalized Reactance Compensation Technique in Wideband Class-E Power Amplifier for Lower High Frequency (HF) Bands

KHAIRUL HILMI YUSOF[1,2], (Member, IEEE), FARID ZUBIR[1,2], (Member, IEEE),
MOHAMAD KAMAL A. RAHIM[2], (Senior Member, IEEE),
NARENDRA KUMAR[3], (Senior Member, IEEE), ZUBAIDA YUSOFF[4], (Senior Member, IEEE),
PETER GARDNER[5], (Senior Member, IEEE), AND THOMAS JOHNSON[6], (Member, IEEE)
[1]Wireless Communication Centre, Faculty of Electrical Engineering, Universiti Teknologi Malaysia, Johor Bahru 81310, Malaysia
[2]Department of Communication Engineering, Faculty of Electrical Engineering, Universiti Teknologi Malaysia, Johor Bahru 81310, Malaysia
[3]Department of Electrical Engineering, Faculty of Engineering, University of Malaya, Kuala Lumpur 50603, Malaysia
[4]Faculty of Engineering, Multimedia University, Persiaran Multimedia, Cyberjaya, Selangor 63100, Malaysia
[5]Department of Electronic, Electrical and Systems Engineering, University of Birmingham, B15 2TT Birmingham, U.K.
[6]Faculty of Applied Science, School of Engineering, The University of British Columbia, Kelowna, BC V1V 1V7, Canada

Corresponding authors: Khairul Hilmi Yusof (khilmi4@graduate.utm.my), Farid Zubir (faridzubir@utm.my), and Zubaida Yusoff (zubaida@mmu.edu.my)

ABSTRACT This paper discussed a systematic design approach for reactance compensated class-E power amplifier. The theory behind conventional Class-E is described then differences between reactance compensation Class-E is explained and derived. The reactance compensated Class-E gives better high efficiency bandwidth. The range of shunt capacitor value that can maintain high efficiency operation also increases compared to conventional Class-E. The overall impedance for reactance compensated Class-E is derived and shows that it is the same as Class-E. The contribution of this paper is to present a high-performance wideband Class-E Power Amplifier in the operating frequency of low MHz range for the first time. Also, a systematic design approach on the theoretical derivation of Class-E Power Amplifiers with reactance compensation method is presented in this work. To verify the design method and simulation results, we fabricated and measured the proposed design. Wideband Class-E Power Amplifier at low MHz frequency is achieved. The results show that all simulation, designing methods and experimental results confirm each other. The theoretical and simulated results of reactance compensated Class-E shows 17.3% and 33.3% increase in high efficiency bandwidth compared to conventional Class-E. The measurement result shows the reactance compensation technique shows an increase in its high efficiency bandwidth by 52.3% compared to conventional Class-E. Reactance compensation can be used to improve the high efficiency bandwidth of conventional Class-E and shows promises in realizing wideband Class-E. As the overall impedance of reactance compensated Class-E is the same as conventional Class-E, implementing this method would simplify the analysis in other high efficiency amplifier topologies like push-pull, Doherty, and Outphasing

INDEX TERMS Wideband, high efficiency, reactance compensation, class-E, switch mode power supply.

The associate editor coordinating the review of this manuscript and approving it for publication was Tae Wook Kim.

I. INTRODUCTION

The Class-E power amplifier is one of the switch mode amplifier (SMPA) that operates in such a way that the signal between voltage and current is non-overlapping [1], [2], [3]. The transistor in SMPA operates as a switch where current and voltages does not overlap each other, resulting in high efficiency operation. For theoretical study, the transistor can be replaced as an ideal switch. A generic Class-E amplifier circuit diagram can be seen in Fig. 1, where C_1 is the shunt capacitor and C_2, L_2 is the resonator, L_s is the phase shift and L_1 as a RF choke. In conventional Class-E analysis discussed in [4] and [5] the harmonic impedance seen by the capacitor combination are open circuits [4]. The harmonic impedance of the Class-E only consist of a shunt capacitor C_1 [6]. As such, it is crucial that C_1 value is chosen correctly.
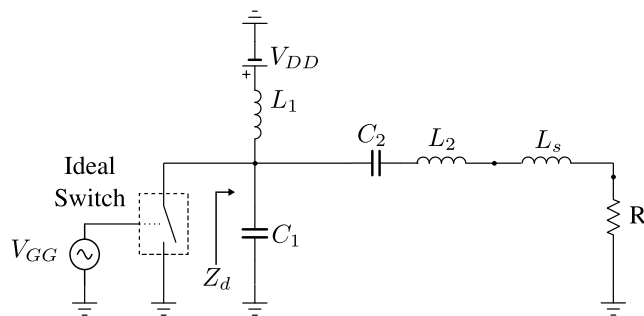

FIGURE 1. Class-E amplifier circuit.

The conventional Class-E has a narrow high efficiency bandwidth. If there is a shift in the input frequency, the efficiency will drop significantly because of the narrowband design. As telecommunication technology grows there is a need of technique that can improve the high efficiency bandwidth of Class-E. Recently, there have been studies that discusses on wideband technique for amplifier such as in [7], [8], [9], and [10]. In [7] low pass filter matching network method was used to achieve wideband Class-E. The low pass filter matching network used in [7] is designed using transmission line stub as it is suitable at GHz range. Our work cannot use transmission line because of practicality. The transmission line would be too long and takes a lot of space. Converting the transmission line to lump elements would also cause problems, this is because to accurately represent an open circuit stub, a lot of elements needed which will contribute to low efficiency as the lump element is lossy.

While in [8] and [11] discusses about continuous Class-E method. The continuous Class-E method used in [8] was derived using complex method and was applied in [12] using outphasing topology. The author in [12] need to derive new equations as the impedance of continuous Class-E method is not the same as conventional Class-E. Complex mathematics is needed in order to derive those equation in [8] and [12]. The reactance compensation method that will be discussed in this paper is simpler and it has the same impedance as conventional Class-E. This approach removes the need for complex derivation of equations should this technique is implemented in high efficiency amplifier topology such as outphasing [13], push-pull and Doherty as compared to more conventional approaches.

In this work, we describe a systematic design approach on the theoretical derivation of Class-E using combined reactance compensation with harmonic termination on circuit level which have not been published elsewhere. The approach could be further adapted and adopted in systems that requires high efficiency operation such as electric car motor, wireless power transfer, and communication devices. We strongly believe that this work has covered the hypothesis, investigation which was supported by the theoretical derivation and/or suggested solution, and circuit model. It is proven by the simulations and show a result that is of value to the community within that area of expertise and a good contribution that enhances the existing body of knowledge towards high performance and reliability of the advanced transmitter architectures based on switched mode power amplifiers. We have also provided comparison of measurement result between conventional Class-E and reactance compensated Class-E.

In conventional Class-E at fundamental frequency, the overall impedance consists of shunt capacitor, C_1 and Ls where C_2, L_2 behave like a short circuit. Then at higher order harmonics, C_2, L_2 behaves like an open circuit and the only component that is left at higher order harmonics is C_1, so, we cannot really pinpoint at what harmonics that C_1 is tackling. C_1 is present in both fundamental frequency and higher order harmonics, thus the value of C_1 is crucial in providing high efficiency at different operating frequency. In this paper, we would also reveal the range of shunt capacitor, C_1 that gives high efficiency for both reactance compensated Class-E and conventional Class-E. The reactance compensation also act like a harmonic termination, thus increasing the efficiency across a wider bandwidth.

The organization of this paper is as follows, first we will discuss the conventional Class-E and its equation, then explanation on reactance compensation method followed by the derivation of all its relevant equations. Next, we will discuss about the theoretical and simulation result between conventional Class-E and reactance compensated Class-E followed by measurement result then finally, conclusion.

II. IDEAL CLASS-E FUNDAMENTAL EQUATIONS

Ideal Class-E has been discussed and derived by Raab, Sokal [4], [5], [14]. Paper by Raab [4] is one of the early references that thoroughly discussed the operation and equation of an Ideal Class-E amplifier. Fig. 2 shows an ideal Class-E amplifier circuit. The maximum power for a class-E amplifier is obtained with 50% duty cycle.

Fig. 2 in [4] shows the relationship between the switch closure, output load voltage, switch voltage and switch current. A 2π period is used as the time base θ. The switch is open for a period of $2y$ and centered at $\theta = \pi/2$. The switch opens at $\theta_0 = \pi/2 - y$ and closes at $\theta_c = \pi/2 + y$. A 50% duty cycle corresponds to $y = \pi/2$ such that $\theta_0 = 0$ and $\theta_c = \pi$.
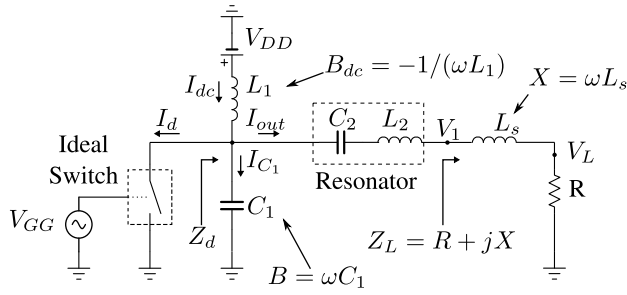
FIGURE 2. Ideal Class-E amplifier circuit with current flows.

Assuming the series resonator composed of C_2 and L_2 has a sufficiently high Q, the load voltage is sinusoidal. Referring to Fig. 2 in [4], the load voltage is defined as

$$v_L(\theta) = c\sin(\theta + \varphi). \tag{1}$$

The sinusoidal load voltage has a zero crossing at $\pi - \varphi$. For a 50% duty cycle, $\varphi = -32.462° = \arctan(-2/\pi)$ [4]. Considering trigonometric relations, we also have [4]

$$\sin\varphi = \frac{-1}{\sqrt{1 + \pi^2/4}}. \tag{2}$$

The load circuit includes a series inductor L_s that modifies the relative phase of the current and voltage at node labeled as v_1. The voltage $v_1(t)$ is sinusoidal at the fundamental switching frequency f and is expressed as

$$v_1(\theta) = c_1\sin(\theta + \varphi + \psi) \tag{3}$$

relative to the load voltage v_0, there is an amplitude change given by

$$c_1 = c\sqrt{1 + \left(\frac{X}{R}\right)^2} \tag{4}$$

and a phase change

$$\psi = \tan\left(\frac{X}{R}\right) \tag{5}$$

where X is the reactance of the inductor L_s at frequency f : $X = 2\pi f L_s$. Raab defines a constant g that depends on duty cycle y and load voltage phase φ [4]

$$g = \frac{y}{\cos\varphi \sin y}. \tag{6}$$

For a 50% duty cycle $y = \pi/2$, $\cos(\psi)$ is [4]

$$\cos(\varphi) = \frac{\pi}{\sqrt{\pi^2 + 4}} \tag{7}$$

and

$$g = \sqrt{1 + \frac{\pi^2}{4}} = 1.8621. \tag{8}$$

The relationship between the effective dc load (R_{dc}) that the amplifier presents to the power supply V_{DD} and the load resistance R at 50% duty cycle is eq. (3.10) in [4]

$$\frac{R_{dc}}{R} = \frac{4 + \pi^2}{8} = 1.7337 \tag{9}$$

By using eq.(3.11) in [4], and evaluated by 50% duty cycle, the shunt susceptance B is

$$B = \frac{2}{\pi\left(1 + \frac{\pi^2}{4}\right)R} = \frac{1}{5.4466R}. \tag{10}$$

This is the susceptance required for the fundamental frequency. From Fig. 2 we know that $B = \omega C_1$, therefore the shunt capacitance C_1 is

$$C_1 = \frac{1}{5.4466\omega R}. \tag{11}$$

From [4], the power factor angle of the load Z_L for a 50% duty cycle is

$$\psi = \arctan\left[\frac{\pi}{8}\left(\frac{\pi^2}{2} - 2\right)\right] = 49.052°. \tag{12}$$

A significant phase shift is required which means the reactance of the series inductor L_s is high. The reactance X can be obtained from the power factor (load impedance) triangle at 50% duty cycle as

$$X = R\tan\psi = 1.1525\,R \tag{13}$$

and substitute $X = \omega L_s$ into (13) gives

$$L_s = \frac{1.1525R}{\omega}. \tag{14}$$

The value of RF choke L_1, resonator C_2,L_2 can be found using equation described in [5] and [14]. It is described in [14] that the value of L_1 should be 10 times or higher than the designed load resistance R, so

$$L_1 = \frac{10R}{\omega}. \tag{15}$$

The series resonator composed of L_2 and C_2 is selected to have sufficiently high Q such that the load current has only one frequency component at the fundamental frequency [14]. It is explained in [9] and [14] that the value of Resonator C_2 can be found using load resistance R and Q factor of the transistor, given by

$$C_2 = \frac{1}{RQ\omega} \tag{16}$$

then L_2 can be found using resonator equation where

$$\omega = \frac{1}{\sqrt{L_2 C_2}} \tag{17}$$

after rearranging (17), we can see that

$$L_2 = \frac{1}{C_2\omega^2} \tag{18}$$

where

$$\omega = 2\pi f$$

We can also derive the overall impedance of the Class-E amplifier, Z_d from the circuit shown in Fig. 1. Y_d is the overall

susceptance, where $Y_d = 1/Z_d$. From circuit diagram in Fig. 1 we can see that

$$Y_d = jB + jB_{dc} + \frac{1}{R + jX} \quad (19)$$

as $B_{dc} = -1/\omega L$, when the value of L_1 is large enough, B_{dc} will become so small that it can be omitted. Resulting in

$$Y_d = jB + \frac{1}{R + jX}. \quad (20)$$

By substituting (10),(13) into (20)

$$
\begin{aligned}
Y_d &= \frac{j}{5.4466R} + \frac{1}{R + j1.525R} \\
&= \frac{1}{R}\left(\frac{j}{5.4466} + \frac{1}{1 + j1.525}\right) \\
&= \frac{1}{R}(0.4295 - j0.3114) \quad (21)
\end{aligned}
$$

substitute $Y_d = 1/Z_d$ into (21) and we get

$$Z_d = (1.526 + j1.1064)R. \quad (22)$$

where Z_d is the overall impedance of conventional Class-E at fundamental frequency [12]. The resonator act like an open circuit impedance at harmonic frequencies, so at harmonic n, Z_d for Class-E at $n = 2, 3 \ldots$ becomes

$$Z_d = -j\frac{5.4466R}{n}. \quad (23)$$

The harmonic impedance on Class-E only consist of C_1. We can see that C_1 is present in both fundamental impedance (22) and harmonic impedance (23), thus showing the importance of choosing the right C_1 value in achieving high efficiency.

III. REACTANCE COMPENSATED CLASS-E

Reactance compensation technique is a method of eliminating the reactance (jX) of the resonator C_2 and L_2. By eliminating the reactance of the resonator, the high efficiency operating bandwidth of a Class-E amplifier can be increased. The compensation element placement can be seen in Fig. 4, where it is placed in parallel with the resonator.

Fig. 3 shows how the compensation element C_p,L_p behaves towards the resonator impedance, where 13.56 MHz is chosen as the designed frequency. imRes is the resonator reactance, and imComp is the reactance of the compensation element and imZnet is the total reactance of both resonator and the compensation element.

As an example, it can be seen from the graph in Fig. 3 that the total reactance imZnet reduces to zero from 13 to 14 MHz. The imComp cancels out the imRes only at a certain frequency, usually somewhere around the design frequency. Without the compensation element, C_p, L_p reactance of the resonator C_2, L_2 reaches zero at its design frequency only,
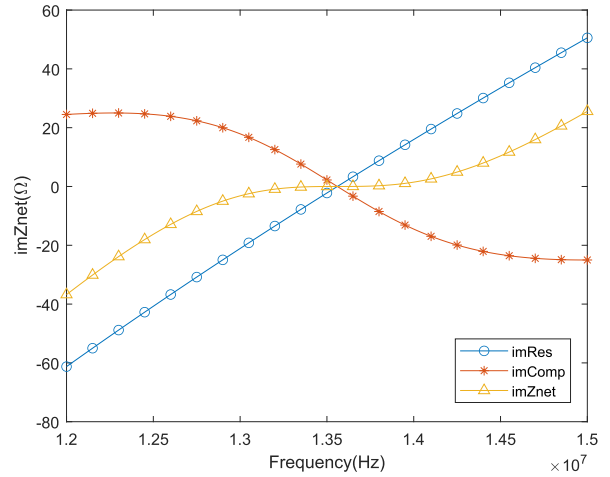

FIGURE 3. Total reactance (imZnet), resonator reactance (imRes) and compensation element reactance (imComp) against frequency.
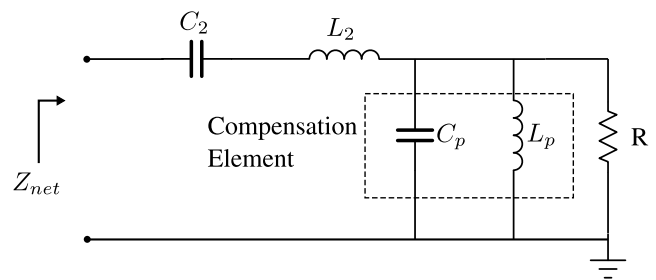

FIGURE 4. Compensation element, C_2, L_2 placement.

which is at 13.56 MHz. In an ideal Class-E, the highest efficiency that can be achieved is at the designed frequency where the reactance value for the resonator is zero. By increasing the bandwidth where the resonator reactance reaches zero, the high efficiency can be maintained over a wider frequency range compared to ideal Class-E

The value of compensation element C_p and L_p can be obtained from the resonator element C_2, L_2. By referring to circuit diagram shown in Fig. 4, the equation for the compensation element C_p, L_p can be derived. Total reactance, $X_{net}(\omega) = \text{imZnet}(\omega)$ is given by

$$
\begin{aligned}
X_{net}(\omega) &= \text{imRes}(\omega) + \text{imComp}(\omega) \\
&= \omega L_2 - \frac{1}{\omega C_2} - \frac{\omega' C_p}{G^2 + (\omega' C_p)^2}.
\end{aligned}
$$

where

$$\omega' = \omega\left(1 - \frac{\omega_0^2}{\omega^2}\right)$$

and $\omega_0 = 1/\sqrt{L_2 C_2} = 1/\sqrt{L_p C_p}$.

Maximum bandwidth with zero reactance can be achieved if

$$\left.\frac{\partial X_{net}(\omega)}{\partial \omega}\right|_{\omega = \omega_0} = 0 \quad (24)$$

$$\left.\frac{\partial X_{net}(\omega)}{\partial \omega}\right|_{\omega=\omega_0}\left(\omega L_2 - \frac{1}{\omega C_2} - \frac{\omega' C_p}{G^2 + (\omega' C_p)^2}\right) = 0 \quad (25)$$

$$L_2 - \frac{1}{\omega^2 C_2} - \frac{2C_p}{G^2} = 0. \quad (26)$$

The values of shunt components L_p and C_p can be obtained through the values of the series components L_2 and C_2 by

$$C_p = L_2 G^2 \quad (27)$$

$$L_p = \frac{C_2}{G^2} \quad (28)$$

We know that $G = 1/R$, then substituting it into (27) and (28) gives

$$C_p = \frac{L_2}{R^2} \quad (29)$$

$$L_p = C_2 R^2 \quad (30)$$

The compensation element C_p, L_p can be calculated from (29) and (30). If we look closely into the equations, C_p value depends on the resonator element L_2 and load resistance R. L_p value depends on resonator element C_2 and load resistance R. Arranging the compensation element C_p, L_p like in Fig. 4 will cancel out the reactance of resonator element C_2, L_2. Total reactance (imZnet) graph in Fig. 3 shows the effect of adding compensation elements.
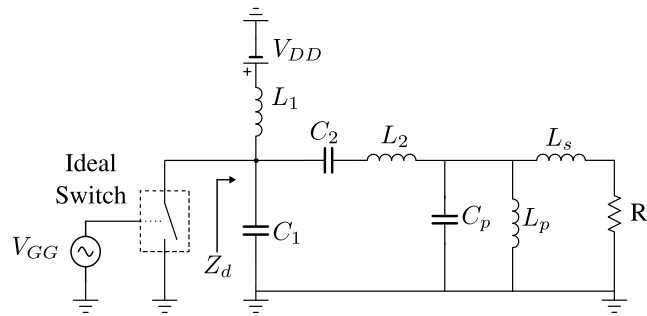

FIGURE 5. Reactance Compensated Class-E circuit diagram.

Earlier in subsection II, the overall impedance of conventional Class-E was derived, next we will derive the overall impedance of reactance compensation method to find out what is the overall impedance of a Class-E amplifier when compensation element is added. By referring to Fig. 5, $Y_d = 1/Z_d$ where Z_d is overall impedance and Y_d is the overall susceptance. Following the same procedure in subsection II we can found that the overall susceptance

$$Y_d = jB + jB_{dc} + jB_p + Y_{LP} + Y \quad (31)$$

$$= jB + jB_p + \frac{1}{jX_{LP}} + \frac{1}{R+jX} \quad (32)$$

$$= \frac{j}{5.4466R} + j\omega C_p + \frac{1}{j\omega L_P} + \frac{1}{R + j1.1525R} \quad (33)$$

substitute (29), (30) into equation (33)

$$Y_d = \frac{j}{5.4466R} + j\omega \frac{L_2}{R^2} + \frac{1}{j\omega C_2 R^2} + \frac{1}{R + j1.1525R} \quad (34)$$

from [9] and [14], we know that

$$C_2 = \frac{1}{RQ\omega} \quad (35)$$

$$L_2 = \frac{RQ}{\omega} \quad (36)$$

then susbstitute (35), (36) into (34) and we get

$$Y_d = \frac{j}{5.4466R} + j\omega \left(\frac{\frac{RQ}{\omega}}{R^2}\right) + \frac{1}{j\omega \frac{R^2}{RQ\omega}} + \frac{1}{R + j1.1525R}$$

$$= \frac{j}{5.4466R} + \frac{jQ}{R} - \frac{jQ}{R} + \frac{1}{R + j1.1525R} \quad (37)$$

both compensation element cancels each other and left with

$$Y_d = \frac{j}{5.4466R} + \frac{1}{R + j1.1525R}$$

$$= \frac{1}{R}\left(\frac{j}{5.4466} + \frac{1}{1 + j1.1525}\right)$$

$$= \frac{1}{R}(0.4295 - j0.3114) \quad (38)$$

knowing that $Y_d = 1/Z_d$, we can solve (38)

$$\frac{1}{Z_d} = \frac{1}{R}(0.4295 - j0.3114)$$

$$Z_d = (1.526 + j1.1064)R. \quad (39)$$

We can see that Reactance Compensated Class-E overall fundamental impedance, Z_d shown in (39) is the same as (22) of the conventional Class-E. This shows that reactance compensation element does not change the overall fundamental impedance of conventional Class-E power amplifier. Harmonic impedance will also be the same as conventional Class-E in (23) because the resonator has an open circuit impedance at harmonic frequencies. So, at harmonic $n = 2, 3 \ldots$

$$Z_d = -j\frac{5.4466R}{n}. \quad (40)$$

One of the performance measures of an amplifier is drain efficiency (η), it can be calculated by using this equation,

$$\eta = \frac{P_{out}}{P_{DC}} \quad (41)$$

where P_{out} is the RF output power and P_{DC} is the DC input power going into the drain. (41) is applicable to both reactance compensation and conventional Class-E power amplifier. By referring to Fig. 5, P_{out} is measured across R and P_{DC} is at drain. All efficiency in this paper is referred to the drain efficiency.

IV. THEORETICAL AND SIMULATED RESULTS AND DISCUSSIONS
In this section, we will discuss the theoretical and simulated results for Class-E and reactance compensated Class-E at 13.56 MHz and 54.24 MHz frequency. Theoretical and simulated Class-E and reactance compensated Class-E was

obtained using LTspice XVII, where an ideal switch model was first used to show theoretical results and then replaced by a transistor model and gate driver to show simulation results.

A. REACTANCE COMPENSATED CLASS-E at 13.56 MHz

Fig. 1 shows the circuit diagram of Class-E using ideal switch. Reactance compensation technique can be applied to the Class-E by adding C_p, L_p as shown in Fig. 5. The values of L_1, C_1, C_2, L_2, C_p, and L_p is calculated by using (11), (14) to (18), (29) and (30). Both circuit diagram is simulated while varying its frequency to find out the bandwidth when the efficiency is above 90%.

From Fig. 6, the original Class-E can achieve 90% efficiency between 12.5 MHz and 15.6 MHz, while reactance compensated Class-E can achieve 90% efficiency between 12 MHz and 16 MHz. However, there is a slight dip in efficiency around 14.5 to 15.5 MHz. The reactance compensated Class-E shows an increase in bandwidth by 17.3% compared to original Class-E.
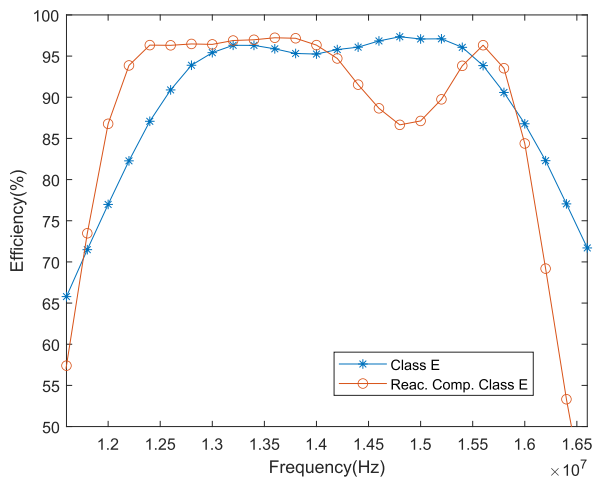

FIGURE 6. Efficiency, η (%) against frequency(Hz) using ideal switch at 13.56MHz.

To better represent the circuit simulation, the circuit diagram is then modified by changing the ideal switch with a real transistor model (EPC2037) provided by the transistor manufacturer and gate driver is used instead of sine wave signal generator. The simulated result for reactance compensated Class-E using real transistor model in Fig. 7 shows 33.3% increase in bandwidth that covers 90% efficiency and above, compared to the original Class-E.

The slight dip occurs when the ideal switch is used, and is consistent at different design frequency (Fig. 12), thus we can conclude that the slight dip is caused by the ideal switch model in LTspice XVII's library itself. The dip disappears when a transistor model is used.

B. SHUNT CAPACITOR RANGE

The shunt capacitor, C_1 in (11) value varies with R and ω, if we keep the resistance R constant at 50 Ω, only ω remains
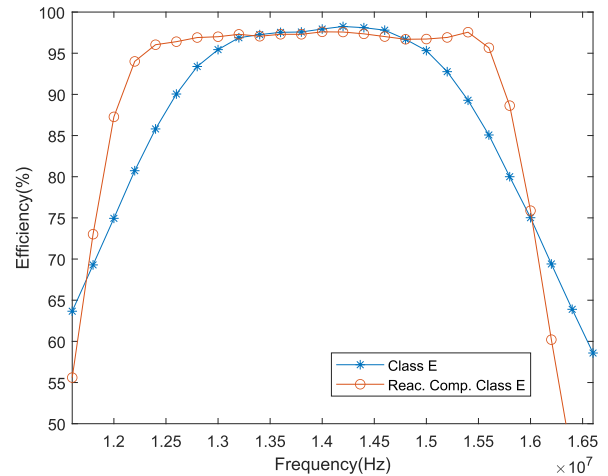

FIGURE 7. Efficiency, η (%) against frequency(Hz) using real transistor at 13.56 MHz.

as a variable that could change C_1. Fig. 8 shows the value of C_1 against efficiency at designed frequency 13.56 MHz using ideal switch, C_1 value that can achieve 90% efficiency is from 15 to 78 pF for Class-E and 16 to 84 pF using reactance compensated Class-E.

There is only slight difference in the range of C_1 between conventional Class-E and Reactance compensated Class-E at 13.56 MHz. This is expected as the reactance at design frequency is zero (refer to Fig. 3) for both conventional and reactance compensation technique.

The behavior of reactance compensated technique is explained in the last section. The reactance of the resonator is compensated and the total reactance reduces to zero from 13 to 14 MHz. It can be seen in Fig. 3 that the total reactance at 12 MHz does not reach zero even after reactance compensation method is applied; however it is closer to zero compared with conventional Class-E. So, to find out the effect of reactance compensation technique towards the range of C_1 at different frequency, the operating frequency is changed to 12 MHz.

Fig. 9 shows C_1 vs efficiency at 12 MHz. The efficiency can reach 90% when C_1 is at 46 pF and above. For conventional Class-E, the maximum efficiency that can be reached is only around 77% at 46 pF. The theoretical result shows reactance compensation method has a significant effect towards C_1 efficiency range.

The circuit in Fig. 5 is changed from ideal switch to real transistor model (EPC2037), same procedure is applied to the circuit and result in Fig. 10 shows the C_1 vs efficiency at 13.56 MHz. From the graph, C_1 value that can achieve 90% efficiency is from 5.4 to 79 pF for Class-E and 7.5 to 85 pF for reactance compensated Class-E. The result shows the same behavior as in Fig. 8, when an ideal switch was used, only slight difference in the range of C_1 between conventional Class-E and Reactance compensated Class-E.

The operating frequency is changed to 12 MHz and the effect of C_1 against efficiency at 12 MHz can be seen
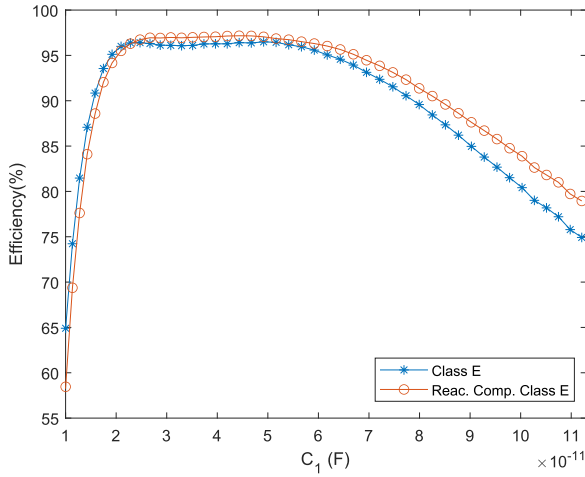
FIGURE 8. Efficiency, η (%) against shunt capacitor, C_1 (F) using ideal switch at 13.56 MHz.
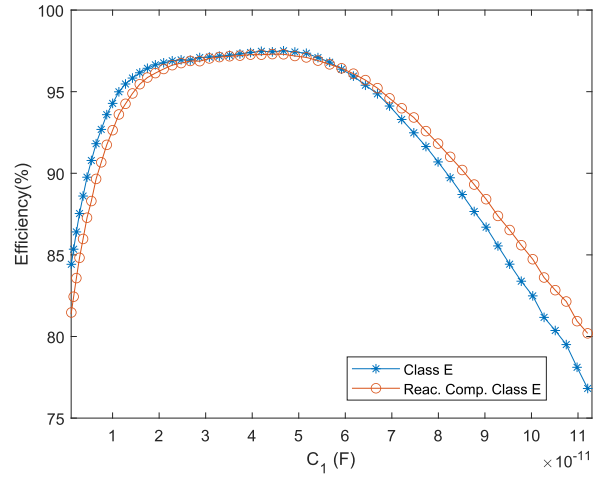

FIGURE 10. Efficiency, η (%) against shunt capacitor, C_1 (F) using real transistor at 13.56 MHz.
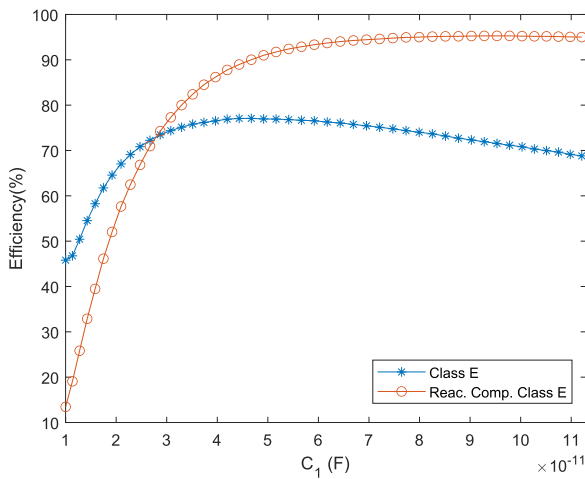

FIGURE 9. Efficiency, η (%) against shunt capacitor, C_1 (F) using ideal switch at 12 MHz.
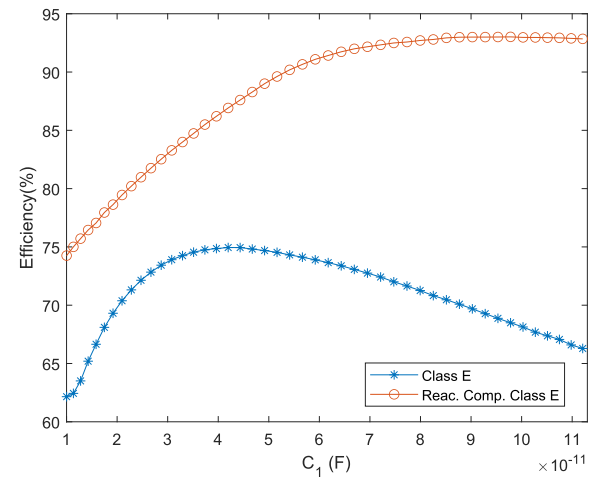

FIGURE 11. Efficiency, η (%) against shunt capacitor, C_1 (F) using real transistor at 12 MHz.

in Fig.11. The behavior of C_1 towards efficiency C_1 value that can reach 90% efficiency is from 54 pF and above. For conventional Class-E, the efficiency can only reach up to 75% at 42 pF. The simulated result in Fig. 10 and Fig. 11 shows reactance compensated method gives significant effect towards C_1 efficiency range. As a summary, the theoretical and simulated result shows reactance compensation technique gives better C_1 efficiency range compared to conventional Class-E.

C. REACTANCE COMPENSATED CLASS-E AT 54.24 MHz
The same design process at 13.56 MHz is repeated at 54.24 MHz, to show whether the same equation for Class-E and reactance compensation technique can be applied at higher frequency. Equation (11), (14) to (18), (29) and (30) is used to calculate all the component values, then the circuit is realized using ideal switch and another circuit is using real transistor model.

Results in Fig. 12 shows that conventional Class-E designed at 54.24 MHz can achieve 90% efficiency between 50 MHz and 61 MHz. By applying reactance compensation technique, we can see that 90% efficiency bandwidth covers from 48 MHz to 63 MHz, it is a 36.4% increase compared to original Class-E. The result for reactance compensation technique using ideal switch at 54.24 MHz behaves similarly with the one designed at 13.56 MHz in Fig. 9. Both have a slight dip in efficiency at certain frequency. The dip happens because of the ideal switch used, which was taken from LTspice XVII's library. However, it disappears when a transistor model (EPC2037) is used. There could be some limitations on the ideal switch in the library as it seems to happen consistently at 13.56 MHz and 54.24 MHz.

Fig. 13 shows the result of Class-E and reactance compensated Class-E using real transistor model. There is an increase by 121% in bandwidth that covers 90% efficiency compared to original Class-E. From the result at 13.56 MHz and 54.24 MHz shown in Fig. 7 and 13 we can conclude the reactance compensated Class-E gives better high efficiency
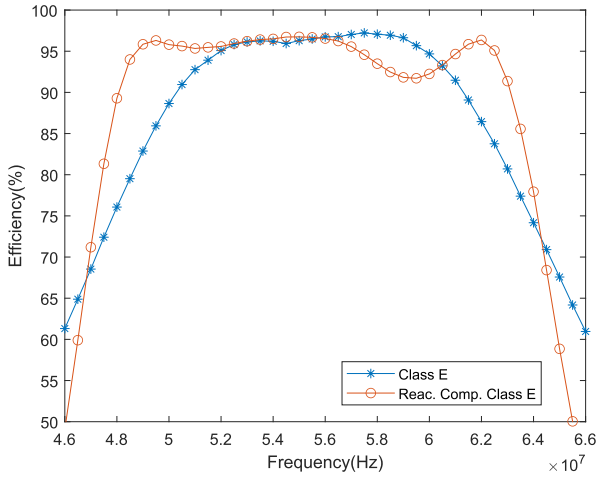
FIGURE 12. Efficiency, η (%) against frequency(Hz) using ideal switch at 54.24 MHz.
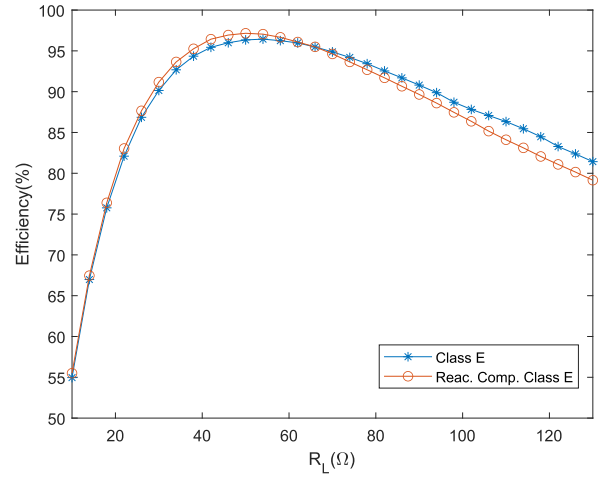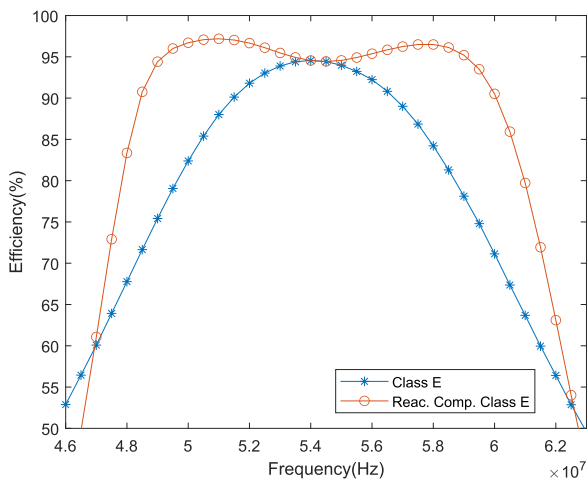

FIGURE 13. Efficiency, η (%) against frequency(Hz) using real transistor at 54.24 MHz.

FIGURE 14. Efficiency, η (%) against load resistance, R_L (Ω) using ideal switch at 13.56 MHz.
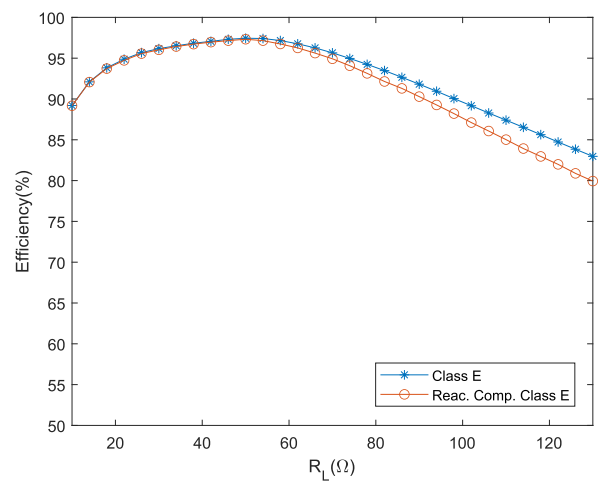

FIGURE 15. Efficiency, η (%) against load resistance, R_L (Ω) using real transistor at 13.56 MHz.

bandwidth at higher frequency compared to lower frequency. If we compare Fig. 7 and 13, at 54.24 MHz the overall shape is different compared to at 13.56 MHz. This is caused by parasitic element and the losses of the transistor, mainly conduction loss and switching losses. This losses is more significant at higher frequency as the transistor switches more frequently.

D. THE EFFECT OF LOAD RESISTANCE TOWARDS EFFICIENCY

In the last section, the frequency is varied to find out the bandwidth that can achieve 90% efficiency, in this section the load resistance, R_L is varied by using the same circuit design as before to find out whether the reactance compensated Class-E behaves differently compared to conventional Class-E in term of efficiency.

The result in Fig. 14 shows that at 13.56 MHz, reactance compensated Class-E behaves similarly compared to conventional Class-E as the load varies from 10 to 130 Ω. This is also true when real transistor model is used, as shown in Fig. 15.

There is only a slight difference in efficiency for reactance compensated Class-E as R_L increased from 80 to 130 Ω.

Next, the design frequency is changed to 54.24 MHz, the result can be seen in Fig. 16. The reactance compensated Class-E behaves similarly compared to conventional Class-E as R_L vary from 10 to 130 Ω, it is almost identical. Changing the ideal switch to real transistor model also shows almost identical result for conventional Class-E and reactance compensated Class-E as shown in Fig. 17.

This shows that the overall impedance of reactance compensated Class-E behaves the same as conventional Class-E, thus proving that fundamental impedance of Class-E in (22) is indeed the same as fundamental impedance of reactance compensated Class-E in (39).

V. CLASS-E AND REACTANCE COMPENSATED CLASS-E AT 27.12 MHz MEASUREMENT RESULT

The simulated circuit in LTspiceXVII is then exported to KiCad 6.0 software for schematics design shown in Fig. 20
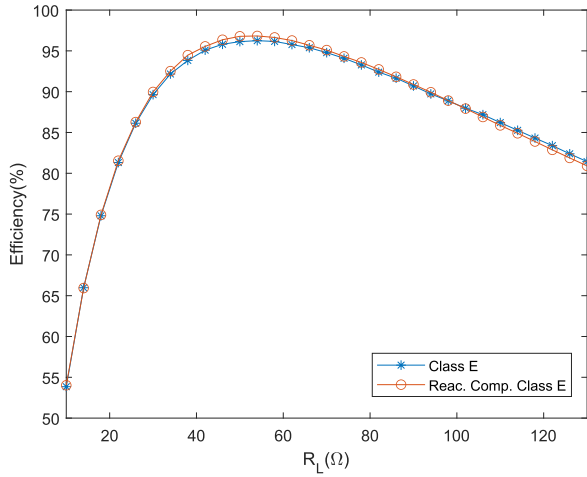
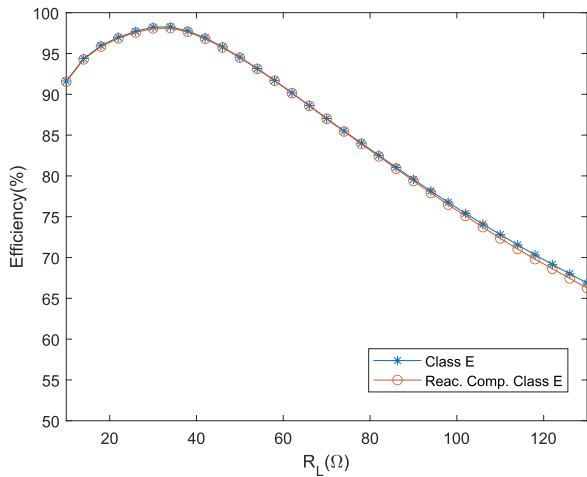**FIGURE 16.** Efficiency, η (%) against load resistance, R_L (Ω) using ideal switch at 54.24 MHz.

FIGURE 17. Efficiency, η (%) against load resistance, R_L (Ω) using real transistor at 54.24 MHz.

FIGURE 18. PCB 3D view front.

FIGURE 19. Fabricated Reactance Compensated Class-E PCB.

followed by PCB layout. The completed PCB layout in 3D view can be seen in Fig. 18, where the gate driver IC (LMG1020) is labeled as IC1 while the transistor (EPC2037) is labeled as Q1. The value of components is rounded up to the closest value available in the market. Table 1 listed the components value used during simulation and measurement. The component was chosen based on the voltage rating and current of the design. From the simulation we can estimate the peak current and voltage in the circuit and choose the most suitable value. The actual fabricated PCB can be seen in Fig. 19.

The PCB layout of reactance compensated Class-E can be referred in Fig. 21. For conventional Class-E, the PCB layout is similar where only the reactance compensation element, L_4, and C_5 is removed. There are some layout design that need to be considered, so that the measured result can be close to the simulated result. The most important consideration is the RF path need to be a short as possible. The components on the
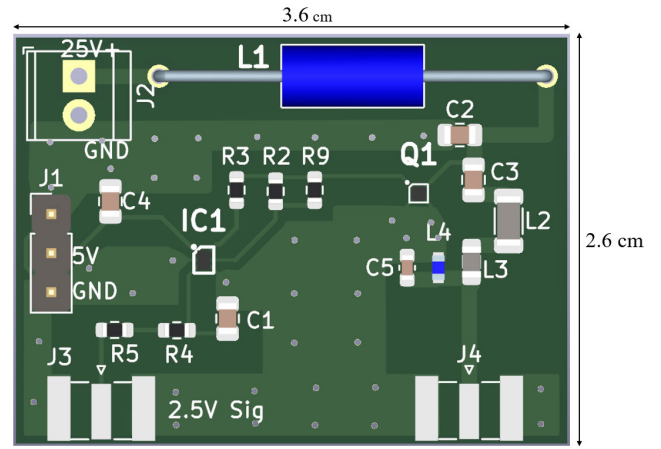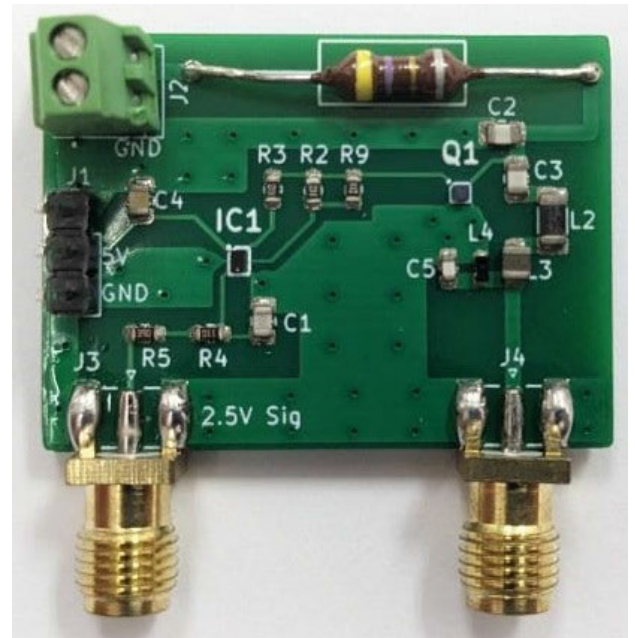
RF path is placed as near as possible without triggering the design rules checker (DRC).

A short path can minimize the effect of inductance in copper traces. Another consideration is the grounding placement of the PCB layout. By removing the ground below RF choke, L_1, the eddy current losses from fields around the inductor can be eliminated. The back of the PCB is filled with ground plane to dissipate the heat of the EPC2037 transistor and provide a way for the component to connect nearest ground. Vias was placed close to the components so that it can have the shortest way to ground.

Output power is measured using a power sensor at the RF output port, J4 and input power is measured at DC input port, J2 using power meter. The efficiency can then be calculated using (41).
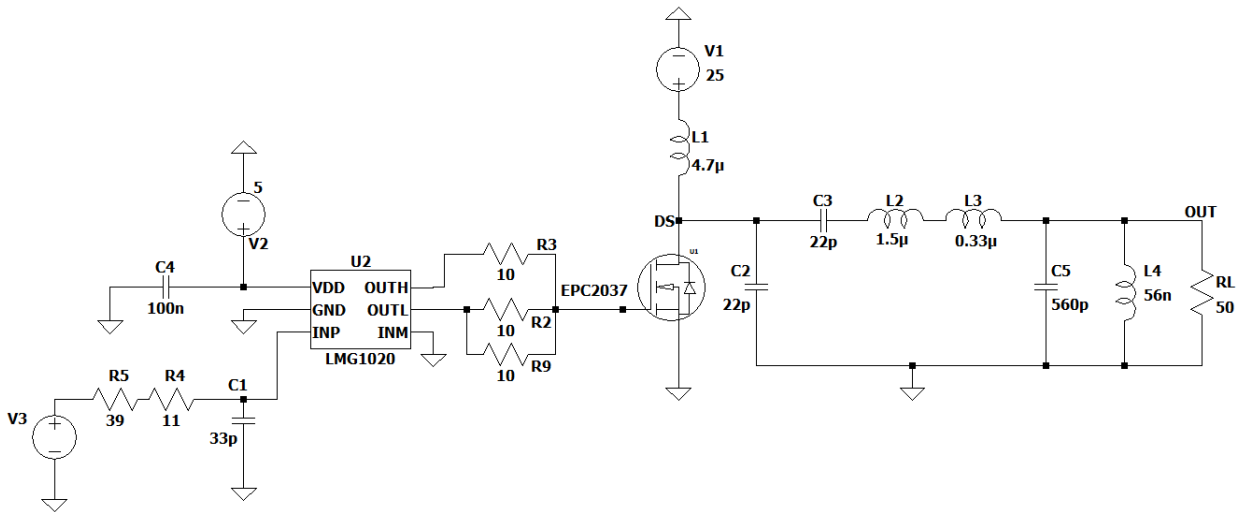
FIGURE 20. The fabricated reactance compensated Class-E schematic diagram, designed at 27.12 MHz.
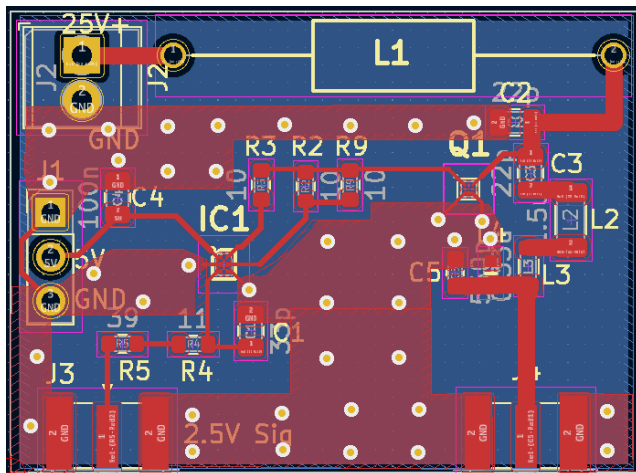

FIGURE 21. PCB layout view front.

TABLE 1. Reactance Compensated Class-E simulation and measurement components value.

Section	Label	Value (simulation)	Value (measurement)
Gate driver (LMG1020) IC1	C1	33 pF	Same as simulation
	C4	100 nF	
	R3	10 Ω	
	R2	10 Ω	
	R4	11 Ω	
	R5	39 Ω	
	R9	10 Ω	
Transistor (EPC2037) Q1	C2	21.5 pF	22 pF
	C3	23.5 pF	22 pF
	C5	586.9 pF	560 pF
	L1	5 μH	4.7 μH
	L2	1.5 μH	1.5 μH
	L3	338.2 nH	0.33 μH
	L4	58.7 nH	56 nH

The measurement result of reactance compensated Class-E at 27.12 MHz can be seen in Fig. 23. The efficiency drop by around 20% as compared to simulated result shown in

TABLE 2. Comparison of Switch-mode Power Amplifier at Lower MHz range for Wireless Power TransferÂ Application.

No	Frequency	Efficiency (%)	Power Level	Technology
[15]	27 MHz	68	3.5 W	GaN
[16]	27 MHz	82	8 W	GaN
[17]	13 MHz	73.4	25.6 W	GaN
[18]	40 MHz	85.9	7.8 W	LDMOS
[19]	27 MHz	74.4	14 W	GaN
This work	25-31 MHz	75	2-18 W	GaN

Fig. 22, this could be because of the additional inductance introduced by the copper traces. Improper grounding could also be the probable cause of decreased efficiency. Effective series resistance (ESR) of each component and the rounded up value could also decrease the efficiency even further. The center frequency of the measurement is shifted a little, this could be due to components value tolerance. A decrease or increase in component value can shift the center frequency.

Fig. 23 shows the measurement result when applying reactance compensation technique. It can be seen that efficiency can be maintained around 75% from 25 to 31 MHz, it is a 52.3% increase as compared to original Class-E which only covers from 26 to 30 MHz.

The measured results shows that the reactance compensation technique can increase the high efficiency bandwidth and operating bandwidth of Class-E power amplifier with minimal component addition and easier implementation as compared to other technique. This technique can be used alongside efficiency enhancement topology like Outphasing. In outphasing topology, the efficiency is maintained when the signal becomes out of phase and output power dropped. The efficiency is maintained over a certain power back-off. Implementing Wideband Class-E will further enhance the Outphasing technique by increasing the high efficiency bandwidth.

The measurement result can be seen in Fig. 24. The overall output power recorded is lower than the
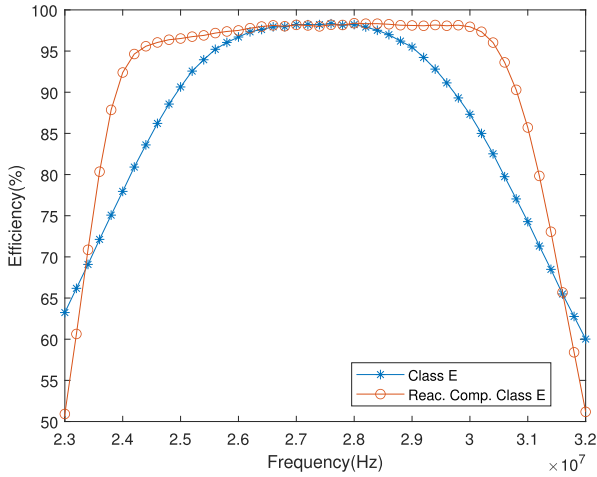
FIGURE 22. Simulation result for efficiency, η (%) against frequency(Hz) at 27.12MHz.
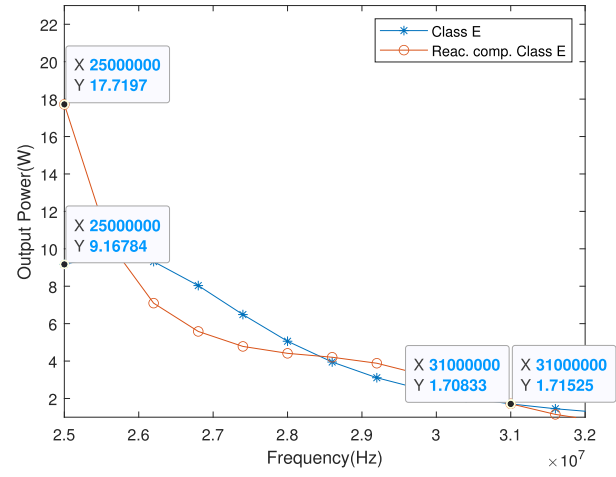

FIGURE 24. Measurement result for output power(W) against frequency(Hz).
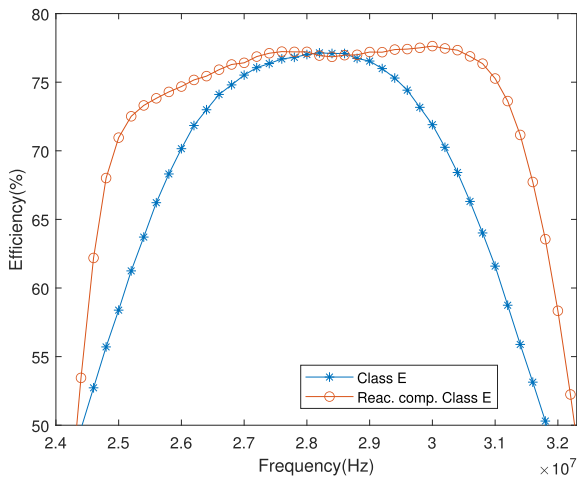

FIGURE 23. Measured result for efficiency, η (%) against frequency(Hz) at 27.12MHz.

simulation result. This could be due to the component and PCB traces losses. From the results, the reactance compensated Class-E still able to achieve 10 dB back-off between 25 MHz and 31 MHz with output power 17.7 W (42.5 dBm) and 1.72 W (32.4 dBm) respectively. However, the conventional Class-E only achieves 7.3 dB back-off between 25 MHz and 31 MHz with 9.17 W (39.6 dBm) and 1.71 W (32.3 dBm) output power. The measurement result shows reactance compensation technique is suitable to be implemented in Outphasing topology as it have the possibility to further enhance the output power back-off.

Table 2 shows the summary of amplifier that was design at similar frequency. Power amplifier in [17], achieved an efficiency up to 73.4% at 25.6 W output power, however it was designed at much lower frequency at 13 MHz and operates at a single frequency. Moreover, the device used in [17] had a voltage rating of 200 V, which explains the reason that it could achieve a higher output power. The device used in this work only have a voltage rating of 100 V. The

reactance compensation technique presented in this work can improve the operating bandwidth of Class E amplifier.

In [19], the efficiency and power level is the closest to this work at 74% and 14 W respectively. However, the design were using conventional Class-E configured as a rectifier, which explains the difference in efficiency with our work. If the design is configured as an amplifier the result would be similar with our conventional Class-E simulation results. Our proposed technique was able to maintain 75% efficiency across 25-31 MHz. This work would benefit certain application where frequency shift most likely happened and efficiency is the main concern. Other work that have similar efficiency an power level is [18]. Their design focuses more on Class-F^{-1} with shunt-shunt inductive power transfer. Implementing Class-F^{-1} is complex, will need a lot of elements. Our design is much simpler and requires less elements. Furthermore, lump elements like capacitor and inductor is lossy, reducing the number of elements can increase the overall efficiency.

Do note that the devices used in [15], [16], [17], [18], and [19] was different compared to this work device (EPC2037), which explain the difference in output power level. A device that is manufactured to operate at high output power would give high power level compared to device that is manufactured at low output power.

VI. CONCLUSION

In this paper, reactance compensation method for Class-E is discussed, and equation regarding the compensation element is derived, followed by the derivation of overall impedance of the reactance Class-E. It is proven theoretically that the overall impedance of the reactance compensated Class-E is the same as Class-E. The theoretical and simulation results of reactance compensated Class-E is discussed and the results shows that there is at least 17.3% increase in high efficiency bandwidth.

The simulation result also shows that at high frequency, reactance compensation gives the most improvement in high efficiency bandwidth as compared to low frequency. The value of R_L is similar with only slight difference between theoretical and simulation results at low and high frequency. As for measurement result, the reactance compensated Class-E shows a 52.3% improvement in high efficiency bandwidth compared to conventional Class-E at 27.12 MHz.

Reactance compensated Class-E shows promises in realizing wideband Class-E. The impedance of reactance compensated Class-E is the same as conventional Class-E. Implementing this method would simplify the impedance analysis in other high efficiency amplifier topology like push-pull, outphasing, and Doherty.

REFERENCES

[1] J. Cumana, A. Grebennikov, G. Sun, N. Kumar, and R. H. Jansen, "An extended topology of parallel-circuit class-E power amplifier to account for larger output capacitances," *IEEE Trans. Microw. Theory Techn.*, vol. 59, no. 12, pp. 3174–3183, Dec. 2011.

[2] N. Kumar, C. Prakash, A. Grebennikov, and A. Mediano, "High-efficiency broadband parallel-circuit class E RF power amplifier with reactance-compensation technique," *IEEE Trans. Microw. Theory Techn.*, vol. 56, no. 3, pp. 604–612, Mar. 2008.

[3] K. Narendra, A. Mediano, L. Anand, and C. Prakash, "Second harmonic reduction in broadband HF/VHF/UHF class E RF power amplifiers," in *IEEE MTT-S Int. Microw. Symp. Dig.*, May 2010, pp. 328–331.

[4] F. Raab, "Idealized operation of the class E tuned power amplifier," *IEEE Trans. Circuits Syst.*, vol. CS-24, no. 12, pp. 725–735, Dec. 1977.

[5] N. O. Sokal and A. D. Sokal, "Class E-A new class of high-efficiency tuned single-ended switching power amplifiers," *IEEE J. Solid-State Circuits*, vol. JSSC-10, no. 3, pp. 168–176, Jun. 1975.

[6] F. H. Raab, "Class-E, class-C, and class-F power amplifiers based upon a finite number of harmonics," *IEEE Trans. Microw. Theory Techn.*, vol. 49, no. 8, pp. 1462–1468, Aug. 2001.

[7] K. Chen and D. Peroulis, "Design of highly efficient broadband class-E power amplifier using synthesized low-pass matching networks," *IEEE Trans. Microw. Theory Techn.*, vol. 59, no. 12, pp. 3162–3173, Dec. 2011.

[8] M. Ozen, R. Jos, and C. Fager, "Continuous class-E power amplifier modes," *IEEE Trans. Circuits Syst. II, Exp. Briefs*, vol. 59, no. 11, pp. 731–735, Nov. 2012.

[9] A. Grebennikov and M. Franco, *Switchmode RF and Microwave Power Amplifiers*. Amsterdam, The Netherlands: Elsevier, 2021.

[10] T. Sharma, P. Aflaki, M. Helaoui, and F. M. Ghannouchi, "Broadband GaN class-E power amplifier for load modulated delta sigma and 5G transmitter applications," *IEEE Access*, vol. 6, pp. 4709–4719, 2018.

[11] Y. M. A. Latha, K. Rawat, and P. Roblin, "Nonlinear embedding model-based continuous class E/F power amplifier," *IEEE Microw. Wireless Compon. Lett.*, vol. 29, no. 11, pp. 714–717, Nov. 2019.

[12] M. Özen, M. van der Heijden, M. Acar, R. Jos, and C. Fager, "A generalized combiner synthesis technique for class-E outphasing transmitters," *IEEE Trans. Circuits Syst. I, Reg. Papers*, vol. 64, no. 5, pp. 1126–1139, May 2017.

[13] A. Ghahremani, A.-J. Annema, and B. Nauta, "Outphasing class-E power amplifiers: From theory to back-off efficiency improvement," *IEEE J. Solid-State Circuits*, vol. 53, no. 5, pp. 1374–1386, May 2018.

[14] N. O. Sokal, "Class E high-efficiency power amplifiers, from HF to microwave," in *IEEE MTT-S Int. Microw. Symp. Dig.*, 1998, pp. 1109–1112.

[15] A. Clements, V. Vishnoi, S. Dehghani, and T. Johnson, "A comparison of GaN class E inverter and synchronous rectifier designs for 13.56 MHz, 27.12 MHz and 40.68 MHz ISM bands," in *Proc. IEEE Wireless Power Transf. Conf. (WPTC)*, Jun. 2018, pp. 1–4.

[16] H. Dadashzadeh, "Design and implementation of class-E power amplifiers and rectifiers for a dual-band capacitive wireless power transfer system," M.S. thesis, Dept. Appl. Sci., School Eng., Univ. British Columbia (Okanagan), Kelowna, BC, Canada, 2022. [Online]. Available: https://open.library.ubc.ca/collections/ubctheses/24/items/1.0406624

[17] W. Chen, R. A. Chinga, S. Yoshida, J. Lin, C. Chen, and W. Lo, "A 25.6 W 13.56 MHz wireless power transfer system with a 94% efficiency GaN class-E power amplifier," in *IEEE MTT-S Int. Microw. Symp. Dig.*, Jun. 2012, pp. 1–3.

[18] T. M. VanderMeulen, "Using canonical filter structures for designing inductive power transfer systems," M.S. thesis, Dept. Appl. Sci., School Eng., Univ. British Columbia (Okanagan), Kelowna, BC, Canada, 2022. [Online]. Available: https://open.library.ubc.ca/collections/ubctheses/24/items/1.0422476

[19] X. Zan and A.-T. Avestruz, "Performance comparisons of synchronous and uncontrolled rectifiers for 27.12 MHz wireless power transfer using CMCD converters," in *Proc. IEEE Energy Convers. Congr. Expo. (ECCE)*, Sep. 2018, pp. 2448–2455.

KHAIRUL HILMI YUSOF (Member, IEEE) received the B.Eng. degree in electrical, majoring in telecommunication and the M.Eng. degree from Universiti Teknologi Malaysia (UTM), in 2013 and 2016, respectively, where he is currently pursuing the Ph.D. degree. He is also a research and development engineer. He is also conducting research into highly efficient wideband power amplifier. His research interests include RF and microwave technologies, including RF amplifier, cognitive radio, and spectrum sensing.

FARID ZUBIR (Member, IEEE) received the B.Eng. degree in electrical, majoring in telecommunication and the M.Eng. degree in RF and microwave from Universiti Teknologi Malaysia (UTM), in 2008 and 2010, respectively, and the Ph.D. degree from the University of Birmingham, U.K., in 2015, for research into direct integration of power amplifiers with antennas in microwave transmitters. He is currently an Assistant Professor with the Department of Communication Engineering, School of Electrical Engineering, UTM. In 2019, he won the scholarship to work as a Honorary Postdoctoral Research Fellow for a period of two years with The University of British Columbia (UBCO), Okanagan, Canada. He is also conducting research into highly efficient and linear amplification power amplifier topology for wireless power systems. His research interests include RF and microwave technologies, including planar array antenna, dielectric resonator antenna (DRA), and active integrated antenna (AIA).

MOHAMAD KAMAL A. RAHIM (Senior Member, IEEE) was born in Alor Setar, Malaysia, in 1964. He received the B.Eng. degree in electrical and electronic engineering from the University of Strathclyde, U.K., in 1987, the master's degree in engineering from The University of New South Wales, Australia, in 1992, and the Ph.D. degree in wideband active antenna from the University of Birmingham, U.K., in 2003. From 1992 to 1999, he was a Lecturer with the Faculty of Electrical Engineering, Universiti Teknologi Malaysia, where he was a Senior Lecturer with the Department of Communication Engineering, from 2005 to 2007. He is currently a professor. His research interests include the design of active and passive antennas, dielectric resonator antennas, microstrip antennas, reflectarray antennas, electromagnetic bandgap, artificial magnetic conductors, left-handed metamaterials, and computer-aided design for antennas.

NARENDRA KUMAR (Senior Member, IEEE) received the Ph.D. degree in electrical engineering from RWTH Technical University Aachen, Aachen, Germany. He has been with Motorola Solutions, since 1999, and held the position of a principal staff engineer in product development and testing. He has been appointed as a Visiting Professor with Istanbul University, since January 2011. Since August 2013, he has been with the Department of Electrical Engineering, University Malaya. He is currently an associate professor. He holds three U.S. patents and four defensive patents in microwave power amplifiers, all assigned to Motorola Solutions. He has authored more than 80 papers in technical journals and conferences and three technical books published in the USA. Since 2011, he has been actively involved in giving technical courses to many organizations in Asia and Europe, including Spain, Germany, Italy, Turkey, and Thailand. His name was included in the 2009 Who's Who in Science and Engineering. His two papers on wideband matching circuits and nonlinear microwave stability were invited papers for IEEE Mediterranean Microwave Symposium 2010 (North Cyprus) and 2012 IEEE Wireless and Microwave Technology Conference (FL, USA). He has been chaired few IEEE and PIERS technical conferences in Europe and Asia, since 2009. He has been conducted few IEEE seminars related to RF and microwave power amplifiers in Europe and Asia, since 2007. He has been serving as a keynote speaker at several IEEE conferences, since 2010. Since June 2009, he has served as a Reviewer for IEEE TRANSACTIONS ON MICROWAVE THEORY TECHNIQUES and *IET Circuit, Devices, and Systems*. He is a fellow of the Institution of Engineering Technology, U.K. He has been appointed to the IEEE Industry Relations Team of Asia–Pacific to support industrial linkage activities, since January 2015. He is also driving industry 4.0 research activities with the collaboration of RWTH Aachen University, Germany, and supporting industry-university relationships in digital transformation.

ZUBAIDA YUSOFF (Senior Member, IEEE) received the B.Sc. degree (cum laude) in electrical and computer engineering and the M.Sc. degree in electrical engineering from The Ohio State University, USA, in 2000 and 2002, respectively, and the Ph.D. degree, in 2012. She holds the position of a Senior Lecturer with the Faculty of Engineering, Multimedia University. She was with Telekom Malaysia International Network Operation, in 2002, before she joined Multimedia University, in 2004. She continued her studies with Cardiff University, Wales, U.K., in 2008. She has presented technical papers at conference nationally and internationally. One of her conference papers has received "Honorable Mention" for the Student Paper Competition at the International Microwave Symposium, USA, in 2011. She has authored/coauthored more than 50 journals and conference papers. Her research interests include power amplifier design, antenna, 5G communications, and analog/mixed signal RF circuit design.

PETER GARDNER (Senior Member, IEEE) received the B.A. degree in physics from the University of Oxford, Oxford, U.K., in 1980, and the M.Sc. and Ph.D. degrees in electrical engineering and electronics from the University of Manchester Institute of Science and Technology (UMIST), Manchester, U.K., in 1990 and 1992, respectively. In 1994, he was a Lecturer with the University of Birmingham, Birmingham, U.K., where he was a Professor of Microwave Engineering, in 2015. He is currently the Head of the Department of Electronic, Electrical and Systems Engineering, Communication and Sensing Research Group, University of Birmingham. His current research interests include theory, technology, applications of the RF, microwave, mm-wave, and terahertz bands.

THOMAS JOHNSON (Member, IEEE) received the B.A.Sc. degree in electrical engineering from The University of British Columbia (UBC), Vancouver, BC, Canada, in 1987, and the M.A.Sc. and Ph.D. degrees from Simon Fraser University, Burnaby, BC, Canada, in 2001 and 2007, respectively, with a focus on research in RF and microwave power amplifiers. Before joining UBC, in 2009, he was a Technical Lead in a number of high-tech companies, including PulseWave RF, Austin, TX, USA, ADC Telecommunications, Vancouver, and Norsat International, Vancouver. He is currently an Associate Professor with the School of Engineering, UBC. He leads the RF and Microwave Technology Research Laboratory, UBC, solving applied problems in the areas of radio frequency and microwave circuits and systems. His research interests include the design of radio frequency circuits and systems, wireless power systems, wireless sensors, and industrial applications of RF/microwave power.

・・・